

Probing the relaxed relaxion and Higgs-portal with S1 & S2

Ranny Budnik,^{1,2,*} Hyungjin Kim,^{1,†} Oleksii Matsedonskyi,^{1,‡} Gilad Perez,^{1,§} and Yotam Soreq^{3,¶}

¹*Department of Particle Physics and Astrophysics,
Weizmann Institute of Science, Rehovot 7610001, Israel*

²*Simons Center for Geometry and Physics and C. N. Yang Institute for Theoretical Physics, SUNY, Stony Brook, NY, USA*

³*Physics Department, Technion—Israel Institute of Technology, Haifa 3200003, Israel*

We study the recent XENON1T excess in context of solar scalar, specifically in the framework of Higgs-portal and the relaxion model. We show that $m_\phi = 1.9 \text{ keV}$ and $g_{\phi e} = 2.4 \times 10^{-14}$ can explain the observed excess in science run 1 (SR1) analysis in the 1-7 keV range. When translated into the scalar-Higgs mixing angle, the corresponding mixing angle $\sin \theta = 10^{-8}$ is intriguingly close to the maximum value of mixing angle for the technical naturalness of the scalar mass. Unlike the solar axion model, the excess favors a massive scalar field because of its softer spectrum. The best fit parameters are in tension with stellar cooling bounds. We furthermore point that the shallow potential of the relaxion implies that the large densities of red giants could naturally destabilise its potential similar to chameleon-type models, potentially suppressing the stellar cooling, albeit for masses of the order of 200 eV or less. This scenario is being currently tested using the S2-only analysis at XENON1T.

I. INTRODUCTION

Recently, the XENON1T experiment reported an excess of electronic recoil events in the SR1 signal [1]. Within the energy range of 1 – 7 keV, the expected number of background only events is 232 ± 15 , while the observed number of events is 285 with an apparent peak near 2 – 3 keV, in contrast to the expected flat background. The discrepancy corresponds to a 3.5σ rejection of the background hypothesis in favor of an additional peaked spectrum resembling a solar axion source [1]. An unaccounted-for background of tritium decay would lower the significance of the excess to about 2.2σ . While it is possible that the excess is due to a statistical fluctuation or yet another unaccounted background, we focus on the case that it is due to the existence of a new degree of freedom with a mass smaller than a few keV.

The interpretation for the excess as a solar axion with $m_a \lesssim 0.1 \text{ keV}$ leads to an electronic coupling of $g_{ae} \sim 3 \times 10^{-12}$, where the corresponding upper bound is $g_{ae} < 3.7 \times 10^{-12}$ [1]. This is consistent with the LUX solar axion search, which implies an upper bound of $g_{ae} < 3.5 \times 10^{-12}$ [2], but in tension with astrophysical bounds from stellar cooling. Ref. [3] reported an upper bound of $g_{ae} \lesssim 3 \times 10^{-13}$ from red giant (RG) stars cooling. Yet, there are hints for a signal in anomalous energy loss in white dwarfs, RG stars and neutron stars which point to a preferred coupling of $g_{ae} = (1.6 \pm 0.3) \times 10^{-13}$ [4] (see also [5]). However, as pointed by Ref. [6], a light scalar with a mass at or below the keV scale can be produced in the Sun and be probed by dark matter (DM) direct

detection experiments through electron ionisation at the keV scale. In this work we mainly focus on this possibility and confront it with the XENON1T excess. Other possible implications of the recent XENON1T data were discussed in [7–33].

Producing a light scalar (or a pseudo-scalar with CP-odd couplings) is generically a non-trivial task from the model-building point of view. We will concentrate on two cases: a generic scalar Higgs-portal scenario, which can be seen as an effective description of various more complicated constructions, and a more predictive relaxion model [34] motivated by the Higgs mass naturalness problem. While the relaxion is considered to be a pseudo-scalar, its vacuum generically breaks CP [35, 36] leading to a scalar-like phenomenology.

Below, we analyse the recent science run 1 XENON1T result [1] in the context of a new scalar field with mass at the keV scale or below and show that such a new particle is compatible with the excess. In addition, we explore its implications for the S2-only analysis [37], and show that such scalar with keV mass has a clear signature in terms of a bump on flat background. However, the bounds from stellar cooling [38] are shown to be stronger and exclude the preferred region of the parameter space. We also consider the case where the tritium background is taken into account and show that the preferred parameter space is consistent with a smaller coupling and the tension with stellar cooling bound is weakened. Finally, we map the relevant parameter space to the relaxion model [34] and also show that the shallow potential of the relaxion, near its first minimum, implies that the RG’s large densities may naturally destabilise the potential, similar to chameleon-type models. We hypothesise that such an effect can ease the stellar cooling bounds by effectively increasing the local relaxion mass in dense stars.

*Electronic address: ran.budnik@weizmann.ac.il

†Electronic address: hyungjin.kim@weizmann.ac.il

‡Electronic address: oleksii.matsedonskyi@weizmann.ac.il

§Electronic address: gilad.perez@weizmann.ac.il

¶Electronic address: soreq@physics.technion.ac.il

II. THE SOLAR RELAXION/SCALAR SIGNAL

We estimate the solar scalar signal by following Ref. [6]. For the axion case, see [39]. The relevant ϕ -electron interaction Lagrangian is given by

$$\mathcal{L} \supset -g_{\phi e} \phi \bar{e} e. \quad (1)$$

Below, we focus on the $m_\phi \lesssim 3$ keV mass range and consider finite mass effects.

Within the Sun, light scalars can be produced by various production mechanisms: bounded electrons (bb), recombination of free electrons (bf), Bremsstrahlung emission due to scatterings of electrons on ions (ff), Bremsstrahlung emission due to scatterings of two electrons (ee) and Compton like processes (C). At the relevant energy scale, the dominant production rate is the electron-ion Bremsstrahlung. The total differential scalar flux is estimated as

$$\frac{d\Phi}{d\omega} \approx \frac{\omega k}{8\pi^3 R^2} \int_{\odot} dV \Gamma^{\text{prod}}(\omega), \quad (2)$$

where Γ^{prod} is sum over all production rates, $R = 1$ AU is the distance between the earth and the Sun, ω and k are the scalar energy and momentum, respectively and V is the Sun volume, where the Sun profile is taken from [40].

The ratio between the matrix elements of a γ emission and a ϕ emission (or absorption) is given by [41]

$$\frac{|\mathcal{M}(e \rightarrow e\phi)|^2}{|\mathcal{M}(e \rightarrow e\gamma)|^2} \approx \frac{g_{\phi e}^2}{4\pi\alpha} \beta^2, \quad (3)$$

where $\beta = k/\omega$ is the scalar velocity. Since the ratio in Eq. (3) enters both in the production and in the detection (divided by β), the ratio between the number of scalar and pseudo scalar events rates can be written as

$$\frac{\mathcal{R}_\phi(\omega)}{\mathcal{R}_a(\omega)} = \frac{g_{\phi e}^4}{g_{ae}^4} \frac{m_e^4}{\omega^4} \left(4 \frac{\beta^2}{3 - \beta^{2/3}} \right)^2, \quad (4)$$

where $\mathcal{R}_{\phi,a}(\omega) = \frac{d\Phi}{d\omega} \sigma_{\phi,a}(\omega)$, and $\sigma_{\phi,a}(\omega)$ is scalar and pseudo scalar absorption cross-section for liquid Xenon [41–43]. From Eq. (4) we learn that the solar scalar signal is softer than the solar axion-like case, and thus, it will be peaked at lower energies.

Next, following [6] we evaluate the $\mathcal{R}_\phi(\omega)\epsilon_{\text{Xe}}$, where the XENON1T detector efficiency, ϵ_{Xe} , is taken from [1]. The detector effects are taken into account by a Gaussian smearing of the signal, where the relevant parameters are adopted from [44]. The predicted ϕ event rates (after smearing) for three benchmark points, BM_{1,2,3}, with $m_\phi = (0, 1.3, 1.9)$ keV and $g_{\phi e} = (0.8, 1.5, 2.4) \times 10^{-14}$, respectively, are plotted in Fig. 1. We validated the smearing procedure by smearing the massless axion signal spectrum from Ref. [39] and comparing it to Fig. 1 of [1], and found a matching up to few percent level.

In addition to the above signal, manifested in both a scintillation signal (S1) and an ionisation signal (S2),

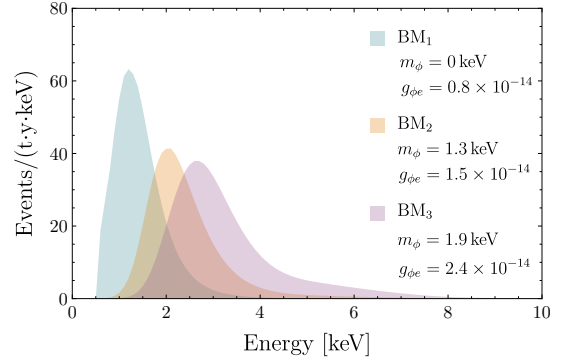


FIG. 1: The solar scalar event rates are shown for three benchmark points as indicated on the plot. The shown event rates include the detector efficiency and resolution. See the main text for details.

we consider the scalar signal in the XENON1T's S2-only analysis [37], where the energy threshold is lower, ~ 200 eV. Since in the scalar case the signal is softer, it is expected to have a better sensitivity in the S2-only analysis. Scalars with masses around the solar interior plasma frequencies, $1 \text{ eV} \lesssim \omega_p \lesssim 300 \text{ eV}$, have enhanced production rate due to mixing with the photon longitudinal mode in the Sun plasma [38]. As pointed out in [6], the resulting sensitivity for $m_\phi \lesssim 300 \text{ eV}$ by using the XENON1T S2-only dataset [37] is improved by an order of magnitude. This resonant production is only efficient for scalar masses below the local plasma frequency, which affects the shape of the expected spectrum with respect to the scalar mass.

III. RECASTING OF THE XENON1T EXCESS AS A RELAXION/SCALAR

We fit the scalar signal for the SR1 dataset of Ref. [1] with and without the tritium background as follows. In the first case, we construct a likelihood function of m_ϕ and $g_{\phi e}$ for the scalar signal and background. We take the background model as fixed, directly from Fig. 4 of [1]. This is justified as the background (without the tritium) is essentially fixed by the high energy spectrum and the injection of the signal at low energy has negligible effect on it. This is evident from the $\sim 2\%$ change at the high end energy tail in the best fit while considering the solar axion, tritium and ν magnetic moment in Ref. [1]. To assess the sensitivity of the result, we also add the tritium background component, where we profile over its magnitude.

By minimize the likelihood, the best fit point (with and without the tritium background) is found to be $m_\phi = 1.9 \text{ keV}$ and $g_{\phi e} = 2.4 \times 10^{-14}$, where the left panel of Fig. 2 shows the 68%, 95% and 99% confidence intervals in the $m_\phi - g_{\phi e}$ plane with and without the tritium background. To find the contours we apply the asymptotic formula from [45] for two free parameters. We find that the preferred region is for a finite

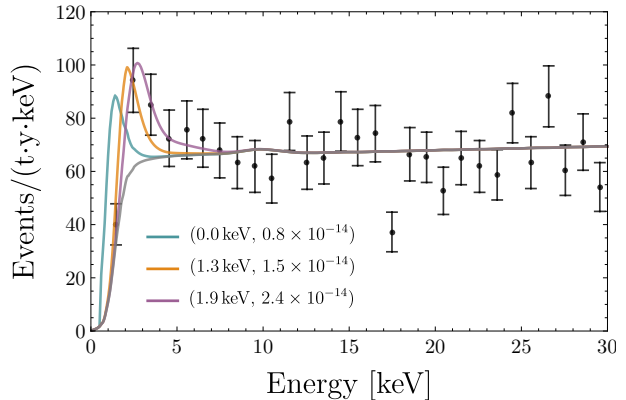
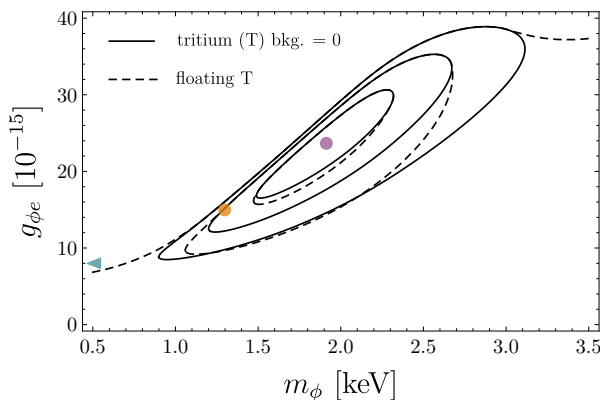


FIG. 2: Left: The 68 %, 95 % and 99 % confidence intervals are shown, solid (dashed) contours are with (without) the tritium background. The three benchmark points with $m_\phi = (0, 1.3, 1.9)$ keV and $g_{\phi e} = (0.8, 1.5, 2.4) \times 10^{-14}$, are marked in cyan, orange and purple, respectively. The purple (BM₃) is the best fit point. Right: The signal+background is shown for the three benchmark points. The black points and gray line are data and background (without tritium) from [1], respectively.

$m_\phi \sim 2$ keV. This is in contrast to the pseudo scalar case, where an effectively massless solution is favored. The reason is that a massless or very light scalar spectrum has a significant soft component relative to the pseudo scalar case, as emphasised in Eq. (4). The right panel of Fig. 2 demonstrates this point, showing a comparison between the signal and background with respect to the XENON1T data for the three benchmark models, BM_{1,2,3}. We note that the preferred region in the parameter space is in tension with the upper bound found from limits on RG cooling including plasmon-scalar mixing effect, $g_{\phi e} < 7 \times 10^{-16}$ [38]. As a cross check, we have performed the same likelihood analysis for the pseudoscalar case and found good agreement with the result of [1].

In addition to the S1 and S2 signal, we now consider the possibility of a scalar signal in the S2-only analysis of XENON1T [37]. This analysis only uses a partial background model, making possible setting upper bounds on signals and testing the consistency of a given signal. In Fig. 3, we plot the S2-only expected signal for BM₂, $m_\phi = 1.3$ keV and $g_{\phi e} = 1.5 \times 10^{-14}$, and compare it to the expected background and the data from [37]. For the purpose of demonstration, we have multiplied the signal by 10. We have also verified that the best fit parameters for SR1 dataset of Ref. [37] is consistent with S2-only analysis. In addition to BM₂, we have also plotted the signals of $m_\phi = 200$ eV and $g_{\phi e} = 4 \times 10^{-15}$. For these parameters, the spectral shape of events for SR1 excess is close to the BM₁ in Fig. 2, while the events at the peak are suppressed by less than ten percent for the same coupling constant. This choice of parameters, especially in the context of relaxed relaxion, may lead to interesting phenomenological consequences inside stellar objects due to finite density corrections to the potential. This will be briefly discussed in Sec. V.

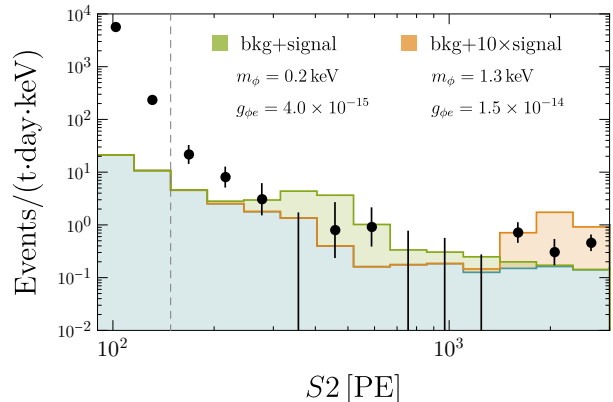


FIG. 3: The signal and background for the S2-only analysis is shown. The BM₂ (orange), $m_\phi = 1.3$ keV and $g_{\phi e} = 1.5 \times 10^{-14}$, is chosen for this plot. The signal is enhanced by 10 for the illustrative purpose. In addition, we have also plotted the signal that would arise from $m_\phi = 200$ eV and $g_{\phi e} = 4 \times 10^{-15}$ (green). Here, the coupling constant is chosen to show the spectrum of events although it is only marginally consistent with the current S2-only analysis [6]. Also, for this choice of mass, the event spectrum for SR1 excess is more or less similar to BM₁ for the same coupling constant. See the main text, especially Sec. V, for the potentially interesting phenomenological consequences related to this choice of parameters.

IV. NATURALNESS MIRACLE

We will now confront the observed excess of events with theoretical models. Let us start with the case of a generic scalar Higgs portal model, containing one new scalar degree of freedom. Its coupling to the electrons comes from the mixing with the Higgs and is given by

$$g_{\phi e} = \frac{\lambda_e}{\sqrt{2}} \sin \theta, \quad (5)$$

where λ_e is the electron Yukawa, and $\sin \theta$ is the mixing whose best-fit value turns out to be $\sin \theta \simeq 1.2 \times 10^{-8}$. In

the absence of any special cosmological dynamics, naturalness implies an upper bound on the ϕ – h mixing angle (the red line in Fig. 4) [46–48]:

$$\sin \theta < \frac{m_\phi}{m_h} \simeq 1.5 \times 10^{-8} \left(\frac{m_\phi}{1.9 \text{ keV}} \right), \quad (6)$$

where in the last equality we used the best-fit value for the scalar mass and $m_h \approx 125 \text{ GeV}$ is the Higgs mass. While the best fit mixing satisfies the naturalness bound, it appears to be strikingly close to the boundary of the natural region. Below we will argue that in fact, in Higgs portal models, having a mixing close to the naturalness bound is much more likely than the mixing taking any given value far below the naturalness bound.

Let us consider a generic Higgs portal potential, featuring a mass mixing term $\mu |H|^2 \phi$, where μ sets the mixing strength. Because of this mixing, the scalar ϕ inherits the Higgs couplings, suppressed by the mixing angle

$$\sin \theta \simeq \mu/v, \quad (7)$$

where v is a Higgs VEV. We also find the following physical ϕ mass around $\phi = 0$

$$m_\phi^2 = m_{\phi 0}^2 - m_h^2 \sin^2 \theta, \quad (8)$$

where $m_{\phi 0}^2$ is the bare ϕ mass. The fact that the XENON1T excess corresponds to $m_\phi^2 \simeq m_h^2 \sin^2 \theta$ means that it can, for instance, be accommodated for $m_\phi^2 \simeq m_{\phi 0}^2 \simeq m_h^2 \sin^2 \theta$, see Eq. (8). However, this requires $\mu \simeq m_{\phi 0}$, and such a relation between the fundamental parameters is not preferred on general grounds, in a sense that it is not as plausible as having $\mu \ll m_{\phi 0}$ or $\mu \gg m_{\phi 0}$ (for definiteness, we assume the likelihood density for the dimension-one parameters values to be uniform on the log scale).

But it turns out that also any model with $\mu \gg m_{\phi 0}$ falls onto the naturalness line to a very good accuracy. With $\mu \gg m_{\phi 0}$ one obtains $\sin \theta \gg m_{\phi 0}/m_h$ and then, according to Eq. (8) the ϕ mass squared becomes negative. The $\phi = 0$ point is unstable and the true minimum is formed where the negative quadratic piece of the potential is compensated by the positive cubic or the quartic. In that minimum the physical ϕ mass is given by the absolute value of the quadratic term coefficient, namely $m_\phi^2 \simeq m_h^2 \sin^2 \theta$. As a result, a neighbourhood of any point $\{m_\phi, \sin \theta\}$ close to the naturalness line corresponds to a large number of particular realisations, which feature almost identical μ parameter, but different $m_{\phi 0}$ satisfying $m_{\phi 0} \ll \mu$. This conclusion is not modified after accounting for quantum corrections.

Yet, turning back to the data, we should conclude that such a generic Higgs portal construction is not capable to avoid the stellar cooling bounds.

V. THE RELAXED RELAXION CASE

Relaxion mechanism [34] allows to explain the smallness of the Higgs mass by a non-trivial cosmological dy-

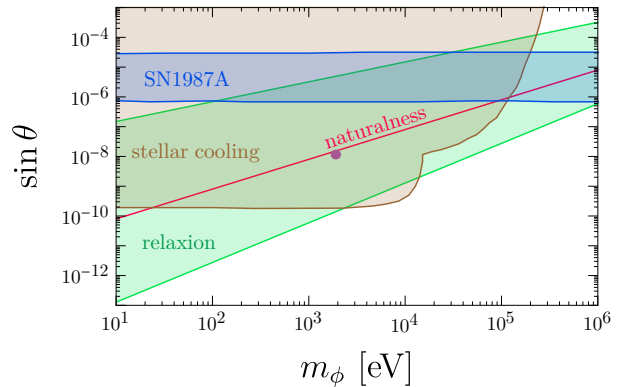


FIG. 4: The best fit to XENON1T excess (purple dot) in terms of the mixing angle, $\sin \theta$, and the scalar mass, m_ϕ , together with the constraints from the stellar cooling [38, 50, 51] (brown), SN1987A [52–54] (blue), as well as preferred relaxion parameter space [49] (green) and the naturalness bound (red). We note that the SN1987A constraint depends on SNe explosion mechanism [55–59].

namics of the Higgs-relaxion system. The same dynamics also relaxes the relaxion mass from its natural value. The relaxion mass and electron coupling are predicted [49]

$$m_\phi^2 \simeq \frac{\Lambda_{\text{br}}^4}{f^2} \frac{\Lambda_{\text{br}}^2}{\Lambda v}, \quad g_{\phi e} = \frac{\lambda_e}{\sqrt{2}} \sin \theta \simeq \lambda_e \frac{\Lambda_{\text{br}}^4}{f v^3}, \quad (9)$$

where Λ is the cutoff, f and Λ_{br} are the period and amplitude of Higgs-dependent barriers, θ is the relaxion-Higgs mixing angle, and $v = 174 \text{ GeV}$ is the Higgs VEV. Assuming $f = \Lambda$ and the SM value for the electron Yukawa coupling $\lambda_e = \lambda_{\text{eSM}}$, we find for the best fit values that

$$\Lambda = f \simeq 60 \text{ TeV}, \quad \Lambda_{\text{br}} \simeq 10 \text{ GeV}. \quad (10)$$

More generally, for $f > \Lambda$ we have a continuum of possibilities, allowing for $\Lambda < 60 \text{ TeV} < f$ and $\Lambda_{\text{br}} > 10 \text{ GeV}$. Furthermore, for $f = \Lambda$, the order of magnitude of the inflationary Hubble parameter is constrained to be within 1 eV and 0.1 GeV . In Fig. 4 we show the position of the excess in the allowed parameter space of the relaxion models (green band), together with relevant experimental bounds.

For the best fit mass, the relaxion model implies the relaxion-Higgs mixing angle is within the range of $\sin \theta \in [10^{-10}, 10^{-5}]$ [49], see Fig. 4. Thus, by relaxing the assumption of $\lambda_e = \lambda_{\text{eSM}}$, we can identify a preferred range for the electron Yukawa to be $10^{-3} < \lambda_e/\lambda_{\text{eSM}} < 10^2$, which is consistent with the current direct upper bound of $\lambda_e \lesssim 600 \times \lambda_{\text{eSM}}$ [60–62].

Finally, we would like to comment on whether the relaxion mechanism can overcome the stellar cooling bounds with a help of a chameleon effect¹. In the relevant mass range, the strongest constraints are derived

¹ Density effects on light particles were also considered in other contexts, see e.g. [63–65].

from the RGs evolution [38], $g_{\phi e} \lesssim 10^{-15}$, and are valid for the relaxion masses $\lesssim 20$ keV. The RG core density significantly exceeds that of the Sun, reaching the nucleon and electron number density $n_{\text{RG}} \sim 10^{15} \text{ eV}^3$ [38, 66], and in principle can affect the local relaxion mass, making the cooling bound inapplicable. The core density contributes to the linear slope of the relaxion potential as $\delta V' \simeq g_{\phi n} n_{\text{RG}}$, where $g_{\phi n}$ is a nucleon-relaxion coupling. This leads to the local field displacement $\delta\phi_{\text{RG}} \simeq \delta V' / m_\phi^2$ which, if large enough, can move the relaxion from the local minimum to one of the subsequent ones, in which case its local mass is expected to increase (one of the possible ways to stop the subsequent relaxion rolling was discussed in Ref. [67, 68]). For this to happen, $\delta\phi_{\text{RG}}$ has to exceed the distance between the minimum and the closest maximum of the relaxion potential, given by $\Delta\phi \simeq \Lambda_{\text{br}}^2 f / \Lambda v$. For $\Lambda = f$ the last expression can be rewritten as $\Delta\phi \simeq \sin\theta v^{5/3} / m_\phi^{2/3}$, so that

$$\frac{\delta\phi_{\text{RG}}}{\Delta\phi} \simeq \frac{g_{\phi n}}{\sin\theta} \frac{n_{\text{RG}}}{m_\phi^{4/3} v^{5/3}} \simeq 10^2 g_{\phi n} \left(\frac{10^{-10}}{\sin\theta} \right) \left(\frac{2 \text{ keV}}{m_\phi} \right)^{4/3} \quad (11)$$

$$\simeq 10^2 g_{\phi n} \left(\frac{2 \text{ keV}}{m_\phi} \right)^{8/3} \quad \text{for } \theta = \theta_{\text{min}}, \quad (12)$$

where in the last equation we showed the result for the minimal mixing allowed for a given relaxion mass. The current experimental bound on proton coupling is $g_{\phi p} \lesssim 10^{-6, -5}$ for $m_\phi = 0.2, 2 \text{ keV}$, respectively [69] (for stronger bounds on coupling to neutrons see [70–73]), and this does not allow in general to obtain $\delta\phi_{\text{RG}} / \Delta\phi > 1$. This last condition however can be satisfied if the local minimum of the relaxion potential is accidentally formed much closer to the maximum than what we assumed in our estimates. Such an option would of course require a significant accidental tuning, of the order 10^{-3} .

However, $\delta\phi_{\text{RG}} / \Delta\phi > 1$ can be naturally achieved for slightly smaller masses. For instance, assuming the coupling $g_{\phi n} = 10^{-6}$, we find that finite-density RG effects can destabilise the relaxion for $m \lesssim 0.2 \text{ keV}$, assuming the minimal allowed mixing, see Eq. (12). If this is the case, the relaxion of 0.2 keV mass could be the source of a potential S2 signal [6] (assuming $\lambda_e \sim 600 m_e / v$ as allowed by the LHC [60–62]), evading the stellar cooling bounds due to the chameleon effect from the couplings to nucleons in RG stars. We have also explicitly checked that such an enhanced value of the coupling to nucleons does not lead to too large quantum corrections to the relaxion potential.

Furthermore, even assuming the standard model couplings to nucleons (electrons), $g_{\phi n} (g_{\phi e}) \sim 10^{-3} (10^{-6}) \sin\theta$, which are automatically present in the original relaxion scenario, we find that the RG density effect can destabilise the relaxion of the mass below $\sim 10^{-5} (10^{-7}) \text{ eV}$, potentially leading to observable effects. Unlike other phenomenological effects of the

relaxion, this one is not dependent on the relaxion-Higgs mixing angle, see Eq. (11). Similar effects in more dense astrophysical objects are expected to appear at even higher relaxion masses. We leave further analysis of this point for future studies.

In summary, we have shown that the reported excess in the SR1 signal is compatible with both generic Higgs portal models and with relaxion models. However, it is difficult to reconcile with the stellar cooling bounds, unless the relaxion minimum is accidentally $\sim 10^3$ times closer to the maximum than it is naturally expected, thus triggering the chameleon effect. On the other hand, the current RG cooling bounds might be naturally eased due to the finite density effects for the relaxion masses $\lesssim 0.2 \text{ keV}$. Such a light relaxion contributes to the S2 signal which has a lower threshold, but it does not explain the SR1 excess.

Acknowledgments

We would like to thank Kfir Blum, Diego Redigolo, and Tomer Volansky for fruitful discussions, and Abhishek Banerjee for technical support. We are grateful to Oz Davidi for his contributions to this project in its initial phase. The work of RB is supported by ISF grant No. 1937/12. RB is the incumbent of the Arye and Ido Dissentshik Career Development Chair. The work of OM is supported by the Foreign Postdoctoral Fellowship Program of the Israel Academy of Sciences and Humanities. The work of GP is supported by grants from The U.S.- Israel Binational Science Foundation (BSF), Israel Science Foundation (ISF), German Israeli Foundation (GIF), Yeda-Sela-SABRA-WRC, and the Segre Research Award. YS is supported by the BSF (NSF-BSF program Grant No. 2018683) and by the Azrieli Foundation. YS is Taub fellow (supported by the Taub Family Foundation).

-
- [1] E. Aprile *et al.*, “Observation of Excess Electronic Recoil Events in XENON1T,” [arXiv:2006.09721 \[hep-ex\]](#).
- [2] LUX Collaboration, D. Akerib *et al.*, “First Searches for Axions and Axionlike Particles with the LUX Experiment,” *Phys. Rev. Lett.* **118** no. 26, (2017) 261301, [arXiv:1704.02297 \[astro-ph.CO\]](#).
- [3] N. Viaux, M. Catelan, P. B. Stetson, G. Raffelt, J. Redondo, A. A. R. Valcarce, and A. Weiss, “Neutrino and axion bounds from the globular cluster M5 (NGC 5904),” *Phys. Rev. Lett.* **111** (2013) 231301, [arXiv:1311.1669 \[astro-ph.SR\]](#).
- [4] M. Giannotti, I. G. Irastorza, J. Redondo, A. Ringwald, and K. Saikawa, “Stellar Recipes for Axion Hunters,” *JCAP* **10** (2017) 010, [arXiv:1708.02111 \[hep-ph\]](#).
- [5] B. M. Hansen, H. Richer, J. Kalirai, R. Goldsbury, S. Frewen, and J. Heyl, “Constraining Neutrino Cooling using the Hot White Dwarf Luminosity Function in the Globular Cluster 47 Tucanae,” *Astrophys. J.* **809** no. 2, (2015) 141, [arXiv:1507.05665 \[astro-ph.SR\]](#).
- [6] R. Budnik, O. Davidi, H. Kim, G. Perez, and N. Priel, “Searching for a solar relaxion or scalar particle with XENON1T and LUX,” *Phys. Rev. D* **100** no. 9, (2019) 095021, [arXiv:1909.02568 \[hep-ph\]](#).
- [7] F. Takahashi, M. Yamada, and W. Yin, “XENON1T anomaly from anomaly-free ALP dark matter and its implications for stellar cooling anomaly,” [arXiv:2006.10035 \[hep-ph\]](#).
- [8] K. Kannike, M. Raidal, H. Veermäe, A. Strumia, and D. Teresi, “Dark Matter and the XENON1T electron recoil excess,” [arXiv:2006.10735 \[hep-ph\]](#).
- [9] G. Alonso-Álvarez, F. Ertas, J. Jaeckel, F. Kahlhoefer, and L. Thormaehlen, “Hidden Photon Dark Matter in the Light of XENON1T and Stellar Cooling,” [arXiv:2006.11243 \[hep-ph\]](#).
- [10] d. Amaral, Dorian Warren Praia, D. G. Cerdeno, P. Foldenauer, and E. Reid, “Solar neutrino probes of the muon anomalous magnetic moment in the gauged $U(1)_{L_\mu-L_\tau}$,” [arXiv:2006.11225 \[hep-ph\]](#).
- [11] B. Fornal, P. Sandick, J. Shu, M. Su, and Y. Zhao, “Boosted Dark Matter Interpretation of the XENON1T Excess,” [arXiv:2006.11264 \[hep-ph\]](#).
- [12] C. Boehm, D. G. Cerdeno, M. Fairbairn, P. A. Machado, and A. C. Vincent, “Light new physics in XENON1T,” [arXiv:2006.11250 \[hep-ph\]](#).
- [13] A. Bally, S. Jana, and A. Trautner, “Neutrino self-interactions and XENON1T electron recoil excess,” [arXiv:2006.11919 \[hep-ph\]](#).
- [14] K. Harigaya, Y. Nakai, and M. Suzuki, “Inelastic Dark Matter Electron Scattering and the XENON1T Excess,” [arXiv:2006.11938 \[hep-ph\]](#).
- [15] L. Su, W. Wang, L. Wu, J. M. Yang, and B. Zhu, “Xenon1T anomaly: Inelastic Cosmic Ray Boosted Dark Matter,” [arXiv:2006.11837 \[hep-ph\]](#).
- [16] M. Du, J. Liang, Z. Liu, V. Q. Tran, and Y. Xue, “On-shell mediator dark matter models and the Xenon1T anomaly,” [arXiv:2006.11949 \[hep-ph\]](#).
- [17] L. Di Luzio, M. Fedele, M. Giannotti, F. Mescia, and E. Nardi, “Solar axions cannot explain the XENON1T excess,” [arXiv:2006.12487 \[hep-ph\]](#).
- [18] U. K. Dey, T. N. Maity, and T. S. Ray, “Prospects of Migdal Effect in the Explanation of XENON1T Electron Recoil Excess,” [arXiv:2006.12529 \[hep-ph\]](#).
- [19] Y. Chen, J. Shu, X. Xue, G. Yuan, and Q. Yuan, “Sun Heated MeV-scale Dark Matter and the XENON1T Electron Recoil Excess,” [arXiv:2006.12447 \[hep-ph\]](#).
- [20] N. F. Bell, J. B. Dent, B. Dutta, S. Ghosh, J. Kumar, and J. L. Newstead, “Explaining the XENON1T excess with Luminous Dark Matter,” [arXiv:2006.12461 \[hep-ph\]](#).
- [21] J. Buch, M. A. Buen-Abad, J. Fan, and J. S. C. Leung, “Galactic Origin of Relativistic Bosons and XENON1T Excess,” [arXiv:2006.12488 \[hep-ph\]](#).
- [22] G. Choi, M. Suzuki, and T. T. Yanagida, “XENON1T Anomaly and its Implication for Decaying Warm Dark Matter,” [arXiv:2006.12348 \[hep-ph\]](#).
- [23] D. Aristizabal Sierra, V. De Romeri, L. Flores, and D. Papoulias, “Light vector mediators facing XENON1T data,” [arXiv:2006.12457 \[hep-ph\]](#).
- [24] G. Paz, A. A. Petrov, M. Tammamaro, and J. Zupan, “Shining dark matter in Xenon1T,” [arXiv:2006.12462 \[hep-ph\]](#).
- [25] H. M. Lee, “Exothermic Dark Matter for XENON1T Excess,” [arXiv:2006.13183 \[hep-ph\]](#).
- [26] A. E. Robinson, “XENON1T observes tritium,” [arXiv:2006.13278 \[hep-ex\]](#).
- [27] Q.-H. Cao, R. Ding, and Q.-F. Xiang, “Exploring for sub-MeV Boosted Dark Matter from Xenon Electron Direct Detection,” [arXiv:2006.12767 \[hep-ph\]](#).
- [28] R. Primulando, J. Julio, and P. Uttayarat, “Collider Constraints on a Dark Matter Interpretation of the XENON1T Excess,” [arXiv:2006.13161 \[hep-ph\]](#).
- [29] A. N. Khan, “Can nonstandard neutrino interactions explain the XENON1T spectral excess?,” [arXiv:2006.12887 \[hep-ph\]](#).
- [30] K. Nakayama and Y. Tang, “Gravitational Production of Hidden Photon Dark Matter in light of the XENON1T Excess,” [arXiv:2006.13159 \[hep-ph\]](#).
- [31] Y. Jho, J.-C. Park, S. C. Park, and P.-Y. Tseng, “Gauged Lepton Number and Cosmic-ray Boosted Dark Matter for the XENON1T Excess,” [arXiv:2006.13910 \[hep-ph\]](#).
- [32] M. Baryakhtar, A. Berlin, H. Liu, and N. Weiner, “Electromagnetic Signals of Inelastic Dark Matter Scattering,” [arXiv:2006.13918 \[hep-ph\]](#).
- [33] H. An, M. Pospelov, J. Pradler, and A. Ritz, “New limits on dark photons from solar emission and keV scale dark matter,” [arXiv:2006.13929 \[hep-ph\]](#).
- [34] P. W. Graham, D. E. Kaplan, and S. Rajendran, “Cosmological Relaxation of the Electroweak Scale,” *Phys. Rev. Lett.* **115** no. 22, (2015) 221801, [arXiv:1504.07551 \[hep-ph\]](#).
- [35] T. Flacke, C. Frugiuele, E. Fuchs, R. S. Gupta, and G. Perez, “Phenomenology of relaxion-Higgs mixing,” *JHEP* **06** (2017) 050, [arXiv:1610.02025 \[hep-ph\]](#).
- [36] K. Choi and S. H. Im, “Constraints on Relaxion Windows,” *JHEP* **12** (2016) 093, [arXiv:1610.00680 \[hep-ph\]](#).
- [37] XENON Collaboration, E. Aprile *et al.*, “Light Dark Matter Search with Ionization Signals in XENON1T,” *Phys. Rev. Lett.* **123** no. 25, (2019) 251801, [arXiv:1907.11485 \[hep-ex\]](#).

- [38] E. Hardy and R. Lasenby, “Stellar cooling bounds on new light particles: plasma mixing effects,” *JHEP* **02** (2017) 033, [arXiv:1611.05852 \[hep-ph\]](#).
- [39] J. Redondo, “Solar axion flux from the axion-electron coupling,” *JCAP* **12** (2013) 008, [arXiv:1310.0823 \[hep-ph\]](#).
- [40] N. Vinyoles, A. M. Serenelli, F. L. Villante, S. Basu, J. Bergström, M. Gonzalez-Garcia, M. Maltoni, C. Peña-Garay, and N. Song, “A new Generation of Standard Solar Models,” *Astrophys. J.* **835** no. 2, (2017) 202, [arXiv:1611.09867 \[astro-ph.SR\]](#).
- [41] I. Avignone, F.T., R. Brodzinski, S. Dimopoulos, G. Starkman, A. Drukier, D. Spergel, G. Gelmini, and B. Lynn, “Laboratory Limits on Solar Axions From an Ultralow Background Germanium Spectrometer,” *Phys. Rev. D* **35** (1987) 2752.
- [42] CUORE Collaboration, F. Alessandria *et al.*, “Search for 14.4 keV solar axions from M1 transition of Fe-57 with CUORE crystals,” *JCAP* **05** (2013) 007, [arXiv:1209.2800 \[hep-ex\]](#).
- [43] M. Pospelov, A. Ritz, and M. B. Voloshin, “Bosonic super-WIMPs as keV-scale dark matter,” *Phys. Rev. D* **78** (2008) 115012, [arXiv:0807.3279 \[hep-ph\]](#).
- [44] XENON Collaboration, E. Aprile *et al.*, “Energy resolution and linearity in the keV to MeV range measured in XENON1T,” [arXiv:2003.03825 \[physics.ins-det\]](#).
- [45] G. Cowan, K. Cranmer, E. Gross, and O. Vitells, “Asymptotic formulae for likelihood-based tests of new physics,” *Eur. Phys. J. C* **71** (2011) 1554, [arXiv:1007.1727 \[physics.data-an\]](#). [Erratum: *Eur.Phys.J.C* **73**, 2501 (2013)].
- [46] F. Piazza and M. Pospelov, “Sub-eV scalar dark matter through the super-renormalizable Higgs portal,” *Phys. Rev. D* **82** (2010) 043533, [arXiv:1003.2313 \[hep-ph\]](#).
- [47] A. Arvanitaki, S. Dimopoulos, and K. Van Tilburg, “Sound of Dark Matter: Searching for Light Scalars with Resonant-Mass Detectors,” *Phys. Rev. Lett.* **116** no. 3, (2016) 031102, [arXiv:1508.01798 \[hep-ph\]](#).
- [48] P. W. Graham, D. E. Kaplan, J. Mardon, S. Rajendran, and W. A. Terrano, “Dark Matter Direct Detection with Accelerometers,” *Phys. Rev. D* **93** no. 7, (2016) 075029, [arXiv:1512.06165 \[hep-ph\]](#).
- [49] A. Banerjee, H. Kim, O. Matsedonskyi, G. Perez, and M. S. Safronova, “Probing the Relaxed Relaxion at the Luminosity and Precision Frontiers,” [arXiv:2004.02899 \[hep-ph\]](#).
- [50] J. Grifols, E. Masso, and S. Peris, “Energy Loss From the Sun and RED Giants: Bounds on Short Range Baryonic and Leptonic Forces,” *Mod. Phys. Lett. A* **4** (1989) 311.
- [51] G. Raffelt, “Limits on a CP-violating scalar axion-nucleon interaction,” *Phys. Rev. D* **86** (2012) 015001, [arXiv:1205.1776 \[hep-ph\]](#).
- [52] M. S. Turner, “Axions from SN 1987a,” *Phys. Rev. Lett.* **60** (1988) 1797.
- [53] J. A. Frieman, S. Dimopoulos, and M. S. Turner, “Axions and Stars,” *Phys. Rev. D* **36** (1987) 2201.
- [54] A. Burrows, M. S. Turner, and R. Brinkmann, “Axions and SN 1987a,” *Phys. Rev. D* **39** (1989) 1020.
- [55] N. Bar, K. Blum, and G. D’Amico, “Is there a supernova bound on axions?,” [arXiv:1907.05020 \[hep-ph\]](#).
- [56] E. M. Burbidge, G. R. Burbidge, W. A. Fowler, and F. Hoyle, “Synthesis of the elements in stars,” *Rev. Mod. Phys.* **29** (Oct, 1957) 547–650. <https://link.aps.org/doi/10.1103/RevModPhys.29.547>.
- [57] W. A. Fowler and F. Hoyle, “Neutrino Processes and Pair Formation in Massive Stars and Supernovae,” *Astrophys. J. Suppl.* **9** (1964) 201–319.
- [58] F. Hoyle and W. A. Fowler, “Nucleosynthesis in Supernovae,” *Astrophys. J.* **132** (1960) 565. [Erratum: *Astrophys.J.* **134**, 1028 (1961)].
- [59] D. Kushnir and B. Katz, “Failure of a neutrino-driven explosion after core-collapse may lead to a thermonuclear supernova,” *Astrophys. J.* **811** no. 2, (2015) 97, [arXiv:1412.1096 \[astro-ph.HE\]](#).
- [60] CMS Collaboration, V. Khachatryan *et al.*, “Search for a standard model-like Higgs boson in the $\mu\mu$ - and e^+e^- decay channels at the LHC,” *Phys. Lett. B* **744** (2015) 184–207, [arXiv:1410.6679 \[hep-ex\]](#).
- [61] W. Altmannshofer, J. Brod, and M. Schmaltz, “Experimental constraints on the coupling of the Higgs boson to electrons,” *JHEP* **05** (2015) 125, [arXiv:1503.04830 \[hep-ph\]](#).
- [62] A. Dery, C. Frugiuele, and Y. Nir, “Large Higgs-electron Yukawa coupling in 2HDM,” *JHEP* **04** (2018) 044, [arXiv:1712.04514 \[hep-ph\]](#).
- [63] R. Balkin, J. Serra, K. Springmann, and A. Weiler, “The QCD Axion at Finite Density,” [arXiv:2003.04903 \[hep-ph\]](#).
- [64] D. B. Kaplan, A. E. Nelson, and N. Weiner, “Neutrino oscillations as a probe of dark energy,” *Phys. Rev. Lett.* **93** (2004) 091801, [arXiv:hep-ph/0401099](#).
- [65] A. Hook and J. Huang, “Probing axions with neutron star inspirals and other stellar processes,” *JHEP* **06** (2018) 036, [arXiv:1708.08464 \[hep-ph\]](#).
- [66] G. Raffelt, *Stars as laboratories for fundamental physics: The astrophysics of neutrinos, axions, and other weakly interacting particles.* 5, 1996.
- [67] N. Fonseca, E. Morgante, R. Sato, and G. Servant, “Axion fragmentation,” *JHEP* **04** (2020) 010, [arXiv:1911.08472 \[hep-ph\]](#).
- [68] N. Fonseca, E. Morgante, R. Sato, and G. Servant, “Relaxion Fluctuations (Self-stopping Relaxion) and Overview of Relaxion Stopping Mechanisms,” *JHEP* **05** (2020) 080, [arXiv:1911.08473 \[hep-ph\]](#).
- [69] S. Alighanbari, G. S. Giri, F. L. Constantin, V. I. Korobov, and S. Schiller, “Precise test of quantum electrodynamics and determination of fundamental constants with hd^+ ions,” *Nature* **581** no. 7807, (2020) 152–158. <https://doi.org/10.1038/s41586-020-2261-5>.
- [70] H. Leeb and J. Schmiedmayer, “Constraint on hypothetical light interacting bosons from low-energy neutron experiments,” *Phys. Rev. Lett.* **68** (1992) 1472–1475.
- [71] V. Nesvizhevsky, G. Pignol, and K. Protasov, “Neutron scattering and extra short range interactions,” *Phys. Rev. D* **77** (2008) 034020, [arXiv:0711.2298 \[hep-ph\]](#).
- [72] Y. Pokotilovski, “Constraints on new interactions from neutron scattering experiments,” *Phys. Atom. Nucl.* **69** (2006) 924–931, [arXiv:hep-ph/0601157](#).
- [73] C. Frugiuele, E. Fuchs, G. Perez, and M. Schlaffer, “Constraining New Physics Models with Isotope Shift Spectroscopy,” *Phys. Rev. D* **96** no. 1, (2017) 015011, [arXiv:1602.04822 \[hep-ph\]](#).